

# Molecular simulation of the shear viscosity and the self-diffusion coefficient of mercury along the vapor-liquid coexistence curve

Gabriele Raabe,<sup>a)</sup> B. D. Todd, and Richard J. Sadus<sup>b)</sup>

Centre for Molecular Simulation, Swinburne University of Technology, P.O. Box 218, Hawthorn, Victoria 3122, Australia

(Received 21 April 2005; accepted 26 May 2005; published online 28 July 2005)

In earlier work [G. Raabe and R. J. Sadus, *J. Chem. Phys.* **119**, 6691 (2003)] we reported that the combination of an accurate two-body *ab initio* potential with an empirically determined multibody contribution enables the prediction of the phase coexistence properties, the heats of vaporization, and the pair distribution functions of mercury with reasonable accuracy. In this work we present molecular dynamics simulation results for the shear viscosity and self-diffusion coefficient of mercury along the vapor-liquid coexistence curve using our empirical effective potential. The comparison with experiment and calculations based on a modified Enskog theory shows that our multibody contribution yields reliable predictions of the self-diffusion coefficient at all densities. Good results are also obtained for the shear viscosity of mercury at low to moderate densities. Increasing deviations between the simulation and experimental viscosity data at high densities suggest that not only a temperature-dependent but also a density-dependent multibody contribution is necessary to account for the effect of intermolecular interactions in liquid metals. An analysis of our simulation data near the critical point yields a critical exponent of  $\beta=0.39$ , which is identical to the value obtained from the analysis of the experimental saturation densities. © 2005 American Institute of Physics. [DOI: 10.1063/1.1955530]

## I. INTRODUCTION

Recently,<sup>1</sup> molecular simulation has been successfully used to predict the phase behavior of mercury. The occurrence of considerable changes in the physical properties of mercury, such as metal-nonmetal transitions, together with a high critical temperature and high toxicity, means that mercury and other liquid metals are challenging systems to investigate experimentally.<sup>2-4</sup> For these systems, molecular simulation could have a valuable role in supplementing experimental data. However, the accuracy of predictions by molecular simulation strongly depends on the intermolecular potential involved, and the determination of a suitable potential for mercury has also proved to be a considerable challenge.

The earliest intermolecular potentials published for mercury were  $(n,m)$  Lennard-Jones potentials fitted to experimental data for gas viscosities or the second virial coefficient.<sup>5,6</sup> These potentials suffer from the inaccuracy of the underlying experimental data and are often only explicitly formulated for the calculation of specific properties. In recent years, several *ab initio* studies of the potential-energy curve of the mercury dimer have been published.<sup>7-11</sup> The *ab initio* intermolecular potential reported by Schwerdtfeger *et al.*<sup>11</sup> can be regarded as the most accurate treatment of the two-body potential-energy curve because it is in good agreement with the most recent and most accurate experimental

spectroscopic data. However, it fails to predict the coexisting vapor and liquid densities and the equilibrium pressure of mercury.<sup>1</sup>

The fact that simulations using an accurate *ab initio* pair potential yield very poor agreement with experiment suggests that the thermophysical properties of mercury are influenced by strongly correlating multibody effects. As higher-body potentials for mercury are not available and including such contributions in a molecular simulation would be computationally prohibitive, we<sup>1</sup> added an effective many-body term to the pair potential of Schwerdtfeger *et al.*<sup>11</sup> Using this multibody contribution, we were able to predict mercury's phase coexistence properties, the heats of vaporization, and the pair distribution functions of mercury with reasonable accuracy.<sup>1</sup>

The aim of this work is to determine whether or not the *ab initio* potential by Schwerdtfeger *et al.*<sup>11</sup> in combination with our empirical multibody contribution can be used to accurately determine the shear viscosity and the self-diffusion coefficient of mercury.

## II. THEORY

### A. Effective multibody intermolecular potential

The latest attempt by Schwerdtfeger *et al.*<sup>11</sup> to determine an accurate intermolecular potential for mercury involved *ab initio* calculations and the addition of a spin-orbital contribution, resulting in a two-body potential-energy curve given by

<sup>a)</sup>On leave from the Institut für Thermodynamik, Technische Universität Braunschweig, Hans-Sommer-Str. 5, 38106 Braunschweig, Germany.

<sup>b)</sup>Author to whom correspondence should be addressed. Electronic mail: rsadus@swin.edu.au

$$u_2(S) = \lambda_E \sum_{j=3}^9 a_{2j} (\lambda_r r)^{-2j} - 45.772 54 r^{-4.269 57} \times \exp(-0.672 64 r). \quad (1)$$

For this potential, the minimum depth is  $\varepsilon/k=525.15$  K and the characteristic distance parameter is  $\sigma=3.14$  Å. The meaning and values of the parameters in Eq. (1) can be taken from Schwerdtfeger *et al.*<sup>11</sup>

Although this potential can be regarded as the most accurate treatment of the two-body potential-energy curve, it fails to yield reasonable results for the coexisting vapor and liquid densities and the equilibrium pressure of mercury. Therefore, it is reasonable to infer that higher-body effects may be required to adequately describe the phase behavior of mercury. In our preceding work,<sup>1</sup> we proposed that an improvement could be achieved by including the nonadditive contributions of multibody effects into the Schwerdtfeger *ab initio* pair potential via an effective  $C_9/r^9$  term. The result was a semiempirical effective potential given by

$$u_n = u_2(S) + \frac{C_9}{r^9} \quad (2)$$

with  $C_9$  and  $r$  in Eq. (2) expressed in terms of a.u.

We previously<sup>1</sup> performed Monte Carlo Gibbs-ensemble simulations for vapor-liquid equilibria (VLE) at different temperatures to determine the values of  $C_9$  required for good agreement with experimental liquid phase densities. We observed<sup>1</sup> a linear dependency for the  $C_9$  values with respect to temperature and were able to accurately fit these values to a simple linear function of  $kT/\varepsilon$ :

$$C_9 = -16\,020.46 - 2823.42 \left( \frac{kT}{\varepsilon} \right). \quad (3)$$

It should be emphasized that no attempt was made in this work to specifically adjust the parameters of Eq. (3) to optimize the agreement for transport properties. Therefore, the simulation results for the shear viscosity and the self-diffusion coefficient reported here are genuine predictions.

## B. Simulation details

The simulations were performed in an  $NVT$  ensemble of  $N=500$  particles. The volume of the simulation box was chosen in such a way that the resulting density corresponded to either the density of the liquid or the vapor phase of the vapor-liquid equilibria (VLE) at the given temperature. Information on the densities of the VLE was taken from the simulation results of our previous work<sup>1</sup> or from experiment.<sup>12</sup> The Gear predictor-corrector scheme<sup>13</sup> was used to integrate the equations of motion, with a reduced time step of  $\Delta t^*=0.001$  for the liquid and dense vapor state points near the critical point, and  $\Delta t^*=0.002$  for vapor state points at low densities. The Gaussian thermostat<sup>13</sup> was used to constrain the kinetic temperature.

The shear viscosity was determined by the Green-Kubo<sup>13,14</sup> method of integrating the autocorrelation function of the off-diagonal elements of the viscous pressure tensor  $P_{\alpha\beta}$  given by

$$P_{\alpha\beta} = \left\langle \frac{1}{V} \left( \sum_i \frac{p_{i\alpha} p_{i\beta}}{m_i} + \sum_i \sum_{j>i} r_{ij\alpha} F_{ij\beta} \right) \right\rangle, \quad (4)$$

where  $p_{i\alpha}$  and  $p_{i\beta}$  are the  $\alpha$  and  $\beta$  components of the momentum of particle  $i$ ,  $r_{ij\alpha}$  is the  $\alpha$  component of the distance between the particles  $i$  and  $j$ , and  $F_{ij\beta}$  is the  $\beta$  component of the force of their interaction. To improve the statistics, we averaged the autocorrelation functions over all independent off-diagonal tensor elements, resulting in

$$\eta = \frac{V}{3kT} \int_0^\infty [\langle P_{xy}(0)P_{xy}(t) \rangle + \langle P_{xz}(0)P_{xz}(t) \rangle + \langle P_{yz}(0)P_{yz}(t) \rangle] dt. \quad (5)$$

The self-diffusion coefficient  $D$  was determined from the Einstein relation<sup>13,14</sup> as the mean-square displacement along the unfolded trajectory of a tracer particle

$$D = \lim_{t \rightarrow \infty} \frac{\langle |\mathbf{r}(t) - \mathbf{r}(0)|^2 \rangle}{6t}. \quad (6)$$

As the diffusion coefficient is a single-particle property, we averaged it over all particles to improve the statistics.

The cutoff distance was set to half the box length, and the long-range corrections<sup>13,14</sup> to the potential energy and the pressure tensor were applied. We assumed the spin-orbital contribution to the potential of Schwerdtfeger *et al.*<sup>11</sup> to be negligible at long distances.<sup>1</sup>

To determine the long-range correction for the shear viscosity, we made use of the relationship between the viscosity and the finite-frequency shear modulus at zero wave vector  $G_\infty(0)$  (Ref. 15)

$$\eta = \tau \cdot G_\infty(0) \quad (7)$$

with  $\tau$  being the Maxwell relaxation time. Following Zwanzig and Mountain,<sup>16</sup>  $G_\infty(0)$  can be determined from the intermolecular potential  $u(r)$  by

$$G_\infty(0) = \rho kT + \frac{2\pi}{15} \rho^2 \int_0^\infty dr g(r) \frac{d}{dr} \left[ r^4 \frac{du}{dr} \right] = G_\infty^{\text{id}}(0) + G_\infty^{\text{res}}(0). \quad (8)$$

Thus, by assuming that the pair distribution function  $g(r) \approx 1$  for  $r > r_{\text{cut}}$ , its long-range correction becomes

$$G_\infty^{\text{LRC}}(0) = \frac{2\pi}{15} \rho^2 \int_{r_{\text{cut}}}^\infty dr \frac{d}{dr} \left[ r^4 \frac{du}{dr} \right]. \quad (9)$$

To calculate the long-range correction of the shear viscosity by

$$\eta^{\text{LRC}} = \tau \cdot G_\infty^{\text{LRC}}(0), \quad (10)$$

we need to determine the relaxation time  $\tau$ . This is done through its definition given by Eq. (7), using the short-range results for viscosity from the Green-Kubo formulation and the short-range value of  $G_\infty(0)$  calculated from Eq. (8) with the upper limit of integration set to  $r_{\text{cut}}$ . This integral can be evaluated numerically or by making use of the fact that for every property  $\langle A \rangle$  in a system of  $N$  particles there is another

property  $a(r_{ij})$  that yields  $\langle A \rangle$  by summation over all pair interactions,<sup>13</sup>

$$\langle A \rangle = \sum_i \sum_{j>i} a(r_{ij}) = \frac{N\rho}{2} \int_0^\infty dr g(r) a(r) 4\pi r^2. \quad (11)$$

Thus, there has to be a property—call it  $\Gamma_\infty^{\text{res}}(0)$ —that yields, summated over all pairs, the residual part of  $G_\infty(0)$

$$\langle G_\infty^{\text{res}} \rangle = \sum_i \sum_{j>i} \Gamma_\infty^{\text{res}}(r_{ij}) = \frac{N\rho}{2} \int_0^\infty dr g(r) \Gamma_\infty^{\text{res}}(r) 4\pi r^2. \quad (12)$$

A comparison with the expression in Eq. (8) leads to

$$\Gamma_\infty^{\text{res}}(r_{ij}) = \frac{1}{15} \frac{\rho}{N} \frac{1}{r_{ij}^2} \frac{d}{dr} \left[ r_{ij}^4 \frac{du}{dr} \right]. \quad (13)$$

This expression is easy to evaluate during the simulation. After a summation over all pairs within  $r_{\text{cut}}$ , and adding the ideal part, we get the short-range value of  $G_\infty(0)$ . As the long-range corrections remain constant throughout the simulation, we determined the Maxwell relaxation time at the end of a run from the ensemble average of the short-range values of  $G_\infty(0)$  and the Green-Kubo viscosity, and added the long-range correction  $\eta^{\text{LRC}}$  given by Eq. (11) afterwards. We found that the long-range correction for the viscosity was smaller than the uncertainties of the short-range viscosity values.

For every state point an equilibration phase of 2 000 000 time steps preceded the actual simulation to relax the system to thermodynamic equilibrium for a given temperature and density. A production run consisted of 2 000 000 time steps for a liquid or dense vapor phase point, and up to 8 000 000 time steps for vapor state points at low densities. During a production run for a liquid or a dense gas point, the off-diagonal elements of the viscous pressure tensor and the mean-square displacement of all particles were stored every tenth time step, and 100 stored values were used to determine the autocorrelation function for the Green-Kubo viscosities. For every single simulation, a graphical inspection of the integral was made to check for a sufficient integration time, i.e., the decay of the autocorrelation function to zero during this time. In the case of low vapor densities, the autocorrelation functions of the pressure tensor elements decay very slowly, resulting in the long simulation runs as mentioned above. The interval of data storage had to be increased to 20 time steps, and 1000–2000 stored values had to be used to determine the integral of the pressure autocorrelation function.

For every state point, ten of the above-described production runs were performed to average the equilibrium properties by using the standard block average technique.<sup>14</sup> Due to the enormous computational effort for simulations at state points in the low-density range, only a few were included.

### III. RESULTS AND DISCUSSION

Our simulation results for shear viscosity in the coexisting liquid and vapor phases of mercury are given in Table I. They are compared with experimental results<sup>17–21</sup> in Fig. 1. The experimental data for shear viscosity are mainly re-

TABLE I. Shear viscosities and self-diffusion coefficients along the vapor-liquid coexistence curve obtained from molecular dynamics simulations using Eq. (2). The uncertainties are quoted as standard errors. Superscripts C denotes the critical point.

$T$ (K)	$\eta^L$ ( $10^{-4}$ Pa s)	$\eta^V$ ( $10^{-4}$ Pa s)	$D^L$ ( $10^{-7}$ m <sup>2</sup> /s)	$D^V$ ( $10^{-7}$ m <sup>2</sup> /s)
669.17	15.108±1.104		0.0295±0.0024	
766.89	12.645±0.818		0.0398±0.0026	
827.26	11.460±0.613		0.0461±0.0036	
1050.30	8.742±0.580	1.055±0.103	0.0757±0.0058	5.9314±0.4245
1155.33	7.841±0.678		0.0913±0.0086	
1260.36	7.335±0.559	1.322±0.125	0.1078±0.0073	3.0773±0.3096
1365.39	6.769±0.424	1.519±0.139	0.1253±0.0126	2.3046±0.1786
1470.42	6.235±0.484		0.1475±0.0117	
1573.15		1.948±0.167		0.9751±0.0812
1575.45	5.418±0.343		0.1815±0.0132	
1663.15	5.400±0.369	2.224±0.129	0.1954±0.0130	0.7304±0.0620
1728.15	4.215±0.254	2.660±0.198	0.2755±0.0228	0.5376±0.0340
1748.15	3.662±0.243	2.945±0.238	0.3452±0.0297	0.4585±0.0272
1749.15	3.602±0.208	2.963±0.248	0.3455±0.0254	0.4449±0.0346
1750.15	3.523±0.203	3.086±0.215	0.3455±0.0254	0.4449±0.0346
1751.15	3.200±0.221 <sup>C</sup>		0.3911±0.0328 <sup>C</sup>	

stricted to temperatures below 900 K. Only a few experimental results<sup>17,21</sup> are available at higher temperatures and these data are inconsistent with each other. In addition to the experimental investigation of the shear viscosities, Tippelkirch *et al.*<sup>21</sup> also used an empirical modification of the Enskog theory that employs the experimental data of the VLE to calculate the shear viscosity curve of mercury along the whole coexistence line. As they found their calculation to be in reasonable agreement with experiment, it provides a useful comparison with our simulation results for the temperature range above 900 K up to the critical point at  $T_C = 1751.15$  K.

The Chapman-Enskog<sup>22,23</sup> solution of the Boltzmann equation yields the shear viscosity  $\eta_0$  of a dilute gas

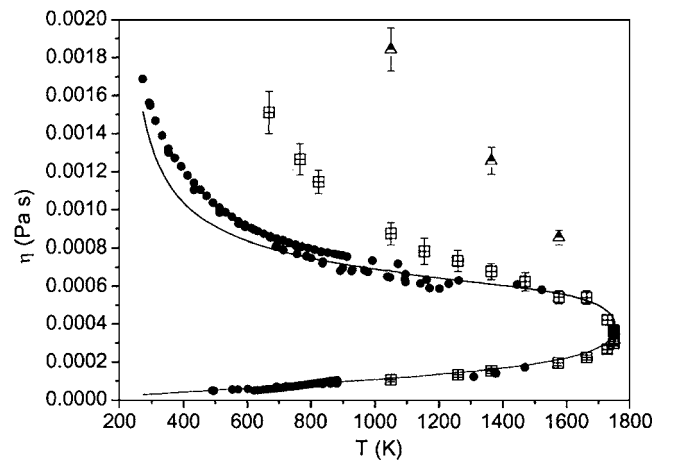


FIG. 1. The comparison of experimental shear viscosity data (Refs. 17–21) (●) for mercury along the saturation line with molecular-dynamics results obtained in this work by using Eq. (2) (◻) and the *ab initio* potential from Schwerdtfeger *et al.* (Ref. 11) (▲). Also shown are the results (—) for the calculation of the shear viscosity based on the empirical modification of the Enskog theory from Eqs. (14)–(20).

$$\eta_0 = \frac{5}{16} \sqrt{\pi m k T} (\pi \sigma^2 \Omega^{(2,2)*})^{-1} \quad (14)$$

with  $m$  being the mass of a molecule. Toppelkirch *et al.*<sup>21</sup> interpreted the product of the characteristic length  $\sigma$  and the collision integral  $\Omega^{(2,2)*}$  as a measure of an effective cross section

$$\sigma^2 \Omega^{(2,2)*} = \sigma_{\text{eff}}^2 \quad (15)$$

and determined a simple temperature dependence of  $\sigma_{\text{eff}}$  for the vapor phase

$$\sigma_{\text{eff}}^v = 4.93 \text{ \AA} \left( \frac{234 \text{ K}}{T} \right)^{0.285} \quad (16)$$

with the melting temperature of mercury  $T_m = 234 \text{ K}$  as a reference. The shear viscosity of the dense gas is then given by the Enskog equation

$$\eta_E^v = \eta_0^v \left( \frac{b^v}{v^v} \right) \left[ \left( \frac{\chi b^v}{v^v} \right)^{-1} + 0.800 + 0.761 \left( \frac{\chi b^v}{v^v} \right) \right]. \quad (17)$$

The quantity  $b$  is the second virial coefficient of a hard-sphere fluid given by

$$b = \frac{2\pi}{3} N_A \sigma_{\text{eff}}^3, \quad (18)$$

where  $N_A$  is the Avogadro constant, and  $v$  is the molar volume. The superscript  $V$  indicates the values of the vapor phase. The Enskog high-density correction  $\chi$  as a function of the molar volume can be taken from Alder and co-workers.<sup>24,25</sup> For a given temperature, the effective hard-sphere diameter in the vapor phase is determined from Eq. (16) to derive the values of the second virial coefficient  $b$  from Eq. (18) and the reference shear viscosity  $\eta_0$  from Eq. (14). Inserting the corresponding molar volume of the vapor phase  $v(T)$  from the experimental VLE data,<sup>12,17,26–28</sup> and  $\chi$  from Alder and co-workers<sup>24,25</sup> yields the shear viscosity of the vapor phase along the saturation line.

The Enskog theory cannot be directly employed for the calculation of shear viscosities at liquid densities because it assumes that the autocorrelation functions decay exponentially. This assumption is not valid at high densities, but Alder and co-workers<sup>24,25</sup> were also able to describe the deviation from Enskog's theory by a correction factor  $F_\eta$  again as a function of the molar volume. Furthermore, Toppelkirch *et al.*<sup>21</sup> determined a different temperature dependence of the effective hard-sphere diameter for the liquid phase to be

$$\sigma_{\text{eff}}^L = 2.81 \text{ \AA} \left( \frac{234 \text{ K}}{T} \right)^{0.0912}. \quad (19)$$

The liquid shear viscosity is then given by

$$\eta^L = \eta_0^L \left( \frac{b^L}{v^L} \right) \left[ \left( \frac{\chi \cdot b^L}{v^L} \right)^{-1} + 0.800 + 0.761 \left( \frac{\chi b^L}{v^L} \right) \right] F_\eta \quad (20)$$

with the superscript  $L$  indicating that  $b$  and  $\eta_0$  have to be recalculated with the  $\sigma_{\text{eff}}$  of the liquid phase. Inserting again  $\chi$  and  $F_\eta$  given by Alder and co-workers<sup>24,25</sup> and experimen-

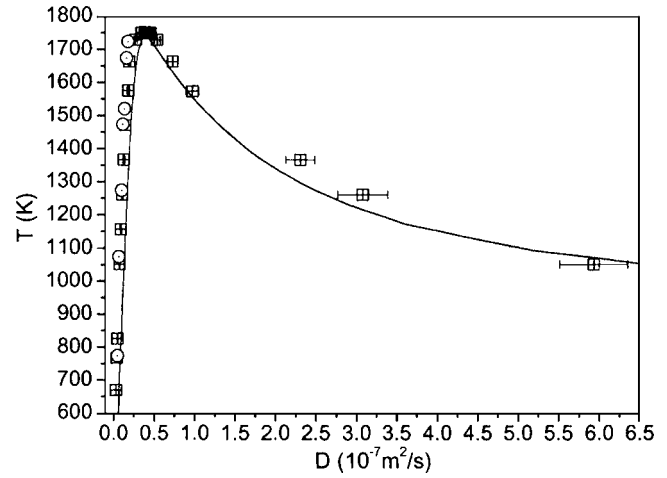


FIG. 2. The comparison of data for the self-diffusion coefficient of mercury along the vapor-liquid coexistence obtained from molecular dynamics (□) by using Eq. (2) with prediction (—) based on the modified Enskog theory from Eqs. (21)–(23), and simulation results and predictions by Belashchenko (Ref. 31) (○).

tal data<sup>12,17,26–28</sup> for  $v^L(T)$  enables the calculation of the shear viscosity along the liquid branch of the coexistence curve. The results of these calculations are depicted as the solid line in Fig. 1.

The comparison of our simulation results for the shear viscosity with experimental data and calculations based on the modified Enskog theory shows that our empirical effective potential yields reasonable predictions of the shear viscosity of mercury over a wide range of state points with low to moderate densities. However, the deviation between the simulation results for the liquid shear viscosity and experiment increases for temperatures below 1400 K, corresponding to state points with densities above 10 000 kg/m<sup>3</sup>. This is understandable in view to the fact that the metal-nonmetal transition occurs in the density range between 9000–11 000 kg/m<sup>3</sup> and noticeably influences the properties of mercury.<sup>2–4</sup> Hensel and co-workers<sup>2–4,21</sup> pointed out that even if it is possible to describe the properties of mercury by an effective pair potential, its nature has to change with density, whereas our empirical multibody contribution only involves a linear temperature dependence. Although it still yields good results for the coexisting vapor and liquid densities and the equilibrium pressure of mercury in Monte Carlo simulations at temperatures below 1400 K,<sup>1</sup> it fails to adequately account for the nature of forces acting in mercury at liquid metal state points. In this region, glue-model approaches,<sup>29,30</sup> that include correlations induced by electron-ion interactions and which have been applied to simulate alkali-fluid properties, may yield a better description. However, Fig. 1 demonstrates that our empirical multibody contribution represents a significant improvement for the prediction of the liquid shear viscosities of mercury compared to the results of the original *ab initio* pair potential.<sup>11</sup>

Our simulation results for the self-diffusion coefficient along the saturation line of mercury are also given in Table I, and they are shown in Fig. 2. In the temperature range in which we performed our simulations, no experimental information on the self-diffusion coefficient is available.

Belanshchenko<sup>31</sup> performed some simulations for the self-diffusion coefficient by employing discrete values of an effective pair potential derived from structural diffraction data. His results may serve as a comparison for the diffusion coefficient in liquid mercury. Additionally, a similar procedure to that used by Toppelkirch *et al.*<sup>21</sup> for the shear viscosity of mercury can be used to calculate the self-diffusion coefficient along the whole VLE saturation line.

The self-diffusion coefficient of a dilute gas is given by<sup>24</sup>

$$D_0 = \frac{0.425v}{N_A \sigma_{\text{eff}}^2} \sqrt{\frac{N_A k T M}{\pi}}, \quad (21)$$

where  $M$  is the molar mass. Again, the Enskog theory relates the self-diffusion coefficient in a dense gas to that of a dilute gas by using the high-density correction<sup>32</sup>

$$D_E^V = D_0^V / \chi. \quad (22)$$

To describe the self-diffusion coefficient in the liquid phase, the deviation from the Enskog theory can likewise be expressed by a correction factor  $F_D$ ,

$$D^L = D_0^L F_D / \chi. \quad (23)$$

With the temperature-dependent hard-sphere diameters  $\sigma_{\text{eff}}^V$  and  $\sigma_{\text{eff}}^L$  and experimental data<sup>12,17,26–28</sup> for the molar volumes of the equilibrium phases, Eq. (21) yields the reference self-diffusion coefficients  $D_0^V$  and  $D_0^L$  for the vapor and liquid phases, respectively. By introducing  $F_D$  and  $\chi$  given by Alder and co-workers,<sup>24,25</sup> the self-diffusion coefficient along the saturation line can be determined from Eqs. (22) and (23).

Figure 2 compares our molecular dynamics simulation results with the calculation of the self-diffusion coefficient as described above, and the simulation results from Belanshchenko.<sup>31</sup> It illustrates that our simulation results are in good agreement with those given by Belanshchenko. Furthermore, our simulation results for the self-diffusion coefficient reproduce the slope of the saturation line in good accordance and consistency with the description given by the modified Enskog theory, even without applying any long-range corrections.

The fact that our empirical effective potential, which was only determined to give good agreement with experimental liquid phase VLE densities, also yields reasonable results for other completely independent properties is an encouraging outcome. The vapor densities,<sup>1</sup> the equilibrium pressures,<sup>1</sup> the pair distribution functions,<sup>1</sup> and now even the shear viscosities and self-diffusion coefficients can be predicted with a reasonable degree of accuracy over a wide range of state points. It suggests that it is maybe possible to account for nonadditive contributions of multibody effects by combining an accurate two-body *ab initio* potential with an empirically determined multibody contribution via an effective term, if the state dependency of this effective term is adequately chosen.

Due to the good results of our simulations near the critical point, we also performed a power-law analysis to deduce the critical exponent from the shape of the coexistence curve for the shear viscosity and the self-diffusion coefficient. It

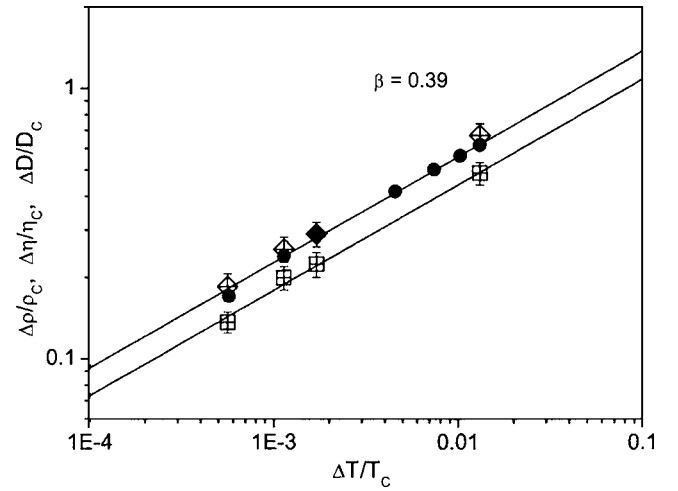


FIG. 3. Scaling law analysis (—) of the shear viscosities (⊞) and the self-diffusion coefficients (⊕) close to the critical point obtained from molecular dynamics by using Eq. (2), and of the coexisting densities obtained from experiment (Ref. 12) (●).

has been shown by Hensel and co-worker<sup>2–4</sup> that the shape of the coexistence curve of the saturated densities of mercury can be well described by the scaling law

$$\rho^L - \rho^V = B \left( \frac{T_C - T}{T_C} \right)^\beta \quad (24)$$

with  $\beta$  experimentally<sup>2–4,12</sup> determined to be 0.36. This value for  $\beta$  is higher than the theoretically derived value of  $\beta = 0.325$  for insulating monoatomic fluids that belong to the universality class of the three-dimensional (3D) Ising model.<sup>2–4,33</sup>

In the same way as for the densities, we determined the critical exponents  $\beta_\eta$  and  $\beta_D$  for a scaling law description of the coexistence curve of the saturated viscosities

$$\eta^L - \eta^V = \beta_\eta \left( \frac{T_C - T}{T_C} \right)^{\beta_\eta} \quad (25)$$

and the self-diffusion coefficients

$$|D^L - D^V| = B_D \left( \frac{T_C - T}{T_C} \right)^{\beta_D}, \quad (26)$$

respectively. We only considered simulation results close to the critical point, i.e., for  $T \geq 1728.15$  or  $\Delta T/T_C \leq 0.0131$ , and obtained  $\beta_\eta = \beta_D = 0.39$ , as shown in Fig. 3. Our value for  $\beta$  is higher than the value of  $\beta = 0.36$  derived by Hensel and co-worker<sup>2–4,12</sup> from the coexisting densities. However, the experimental data used by Hensel and co-worker in their analysis covered a much wider temperature range of  $T = 1073.15–1751.15$  K. As shown in Fig. 3, if the analysis is repeated using saturation densities reported by Götzlaff<sup>12</sup> for the same temperature range (i.e.,  $T \geq 1728.15$  K), a value of  $\beta = 0.39$  is obtained, which is identical to our simulation results.

## IV. CONCLUSIONS

In this work an accurate two-body *ab initio* potential by Schwerdtfeger *et al.*<sup>11</sup> in combination with an empirically

determined multibody contribution, adjusted to liquid densities of the vapor-liquid equilibria only, was used to predict the shear viscosities and the self-diffusion coefficients of mercury along the saturation line. The results were compared with experimental data and simulation results available and calculations based on an empirical modification of the Enskog theory that involves experimental data for the VLE. Increasing deviations between simulation and experiment indicate that not only a temperature-dependent but also a density-dependent multibody contribution is necessary to reliably predict the viscosity of liquid mercury in metal state points with high densities. However, the reasonably good results for the self-diffusion coefficient and the shear viscosity at moderate densities suggest that it is worthwhile to extend efforts on incorporating the effect of the multibody interactions in *ab initio* pair potentials via state-dependent correction terms.

## ACKNOWLEDGMENTS

We thank the Australian Partnership for Advanced Computing and the computer centre of the TU Braunschweig for generous allocations of computing time.

<sup>1</sup>G. Raabe and R. J. Sadus, *J. Chem. Phys.* **119**, 6691 (2003).

<sup>2</sup>F. Hensel, *Adv. Phys.* **44**, 3 (1995).

<sup>3</sup>F. Hensel, *J. Non-Cryst. Solids* **312-314**, 1 (2002).

<sup>4</sup>F. Hensel and W. W. Warren, Jr., *Fluid Metals: The Liquid-Vapor Transition of Metals* (Princeton University Press, Princeton, NJ, 1999).

<sup>5</sup>R. C. Reid, J. M. Prausnitz, and B. E. Poling, *The Properties of Gases and Liquids*, 4th ed. (McGraw-Hill, New York, 1987).

<sup>6</sup>B. Stefanov, O. Iordanov, and L. Zarkova, *J. Phys. B* **15**, 239 (1982).

<sup>7</sup>M. Dolg and H.-J. Flad, *J. Phys. Chem.* **100**, 6147 (1995).

<sup>8</sup>C. F. Kunz, C. Hättig, and B. A. Hess, *Mol. Phys.* **89**, 139 (1996).

<sup>9</sup>A. Bonechi and M. Moraldi, *J. Chem. Phys.* **14**, 5880 (1998).

<sup>10</sup>L. J. Munro, J. K. Johnson, and K. D. Jordan, *J. Chem. Phys.* **114**, 5545 (2001).

<sup>11</sup>P. Schwerdtfeger, R. Wesendrup, G. E. Moyano, A. J. Sadlej, J. Grief, and F. Hensel, *J. Chem. Phys.* **115**, 7401 (2001).

<sup>12</sup>W. Götzlaff, Ph.D. thesis, Philipps-Universität Marburg, Germany, 1988.

<sup>13</sup>M. P. Allen and D. J. Tildesley, *Computer Simulation of Liquids* (Clarendon, Oxford, 1987).

<sup>14</sup>R. J. Sadus, *Molecular Simulation of Fluids: Theory, Algorithms and Object-Oriented* (Elsevier, Amsterdam, 1999).

<sup>15</sup>D. M. Heyes, *The Liquid State: Applications of Molecular Simulations*, (Wiley Chichester, 1998).

<sup>16</sup>R. Zwanzig and R. D. Mountain, *J. Chem. Phys.* **43**, 4464 (1965).

<sup>17</sup>G. Liessmann, W. Schmidt, and S. Reiffarth, *Data Compilation of the Saechsische Olefinwerke Boehlen* (Germany, 1995).

<sup>18</sup>C. Chalilov, *Zh. Tekh. Fiz.* **8**, 1449 (1938).

<sup>19</sup>T. N. Sumarokova and E. N. Berger, *Zh. Prikl. Khim. (S.-Peterburg)* **70**, 1432 (1997).

<sup>20</sup>M. Trautz, *J. Prakt. Chem.* **162**, 218 (1943).

<sup>21</sup>H. v. Toppelkirch, E. U. Franck, F. Hensel, and J. Kestin, *Ber. Bunsenges. Phys. Chem.* **79**, 889 (1975).

<sup>22</sup>J. O. Hirschfelder, C. F. Curtiss and R. B. Bird, *Molecular Theory of Gases and Liquids* (Wiley, New York, 1965).

<sup>23</sup>S. Chapman and T. G. Cowling, *The Mathematical Theory of Nonuniform Gases* (Cambridge University Press, London, 1970).

<sup>24</sup>J. H. Dymond and B. J. Alder, *J. Chem. Phys.* **45**, 2061 (1966).

<sup>25</sup>B. J. Alder, D. M. Gass, and T. E. Wainwright, *J. Chem. Phys.* **53**, 3813 (1970).

<sup>26</sup>N. B. Vargaftik, Y. K. Vinogradov, and V. S. Yargin, *Handbook of Physical Properties of Liquid and Gases*, 3rd ed. (Begell House, Inc., New York, 1996).

<sup>27</sup>N. Mehdipour and A. Boushehri, *Int. J. Thermophys.* **18**, 1329 (1997).

<sup>28</sup>S. Sugawara, T. Sato, and T. Minamiyama, *Bull. JSME* **5**, 711 (1962).

<sup>29</sup>M. Reinaldo-Falagán, P. Tarazona, E. Chacon, E. Velasco, and J. P. Hernandez, *Phys. Rev. B* **67**, 024209 (2003).

<sup>30</sup>E. Chacón, M. Reinaldo-Falagán, P. Tarazona, E. Velasco, and J. P. Hernandez, *Phys. Rev. B* **71**, 024204 (2005).

<sup>31</sup>D. K. Belashchenko, *High Temp.* **40**, 212 (2002).

<sup>32</sup>P. Ascarelli and A. Paskin, *Phys. Rev.* **165**, 222 (1968).

<sup>33</sup>H. Kohno and M. Yao, *J. Phys.: Condens. Matter* **14**, 171 (2002).

The Journal of Chemical Physics is copyrighted by the American Institute of Physics (AIP). Redistribution of journal material is subject to the AIP online journal license and/or AIP copyright. For more information, see <http://ojps.aip.org/jcpof/jcpcr/jsp>